University Library

MINERVA ACCESS

A gateway to Melbourne's research publications

Minerva Access is the Institutional Repository of The University of Melbourne

Author/s:
Lau, CL;Kovacevic, M;Tingleff, TS;Forsythe, JS;Cate, HS;Merlo, D;Cederfur, C;Maclean, FL;Parish, CL;Horne, MK;Nisbet, DR;Beart, PM

Title:
3D Electrospun scaffolds promote a cytotrophic phenotype of cultured primary astrocytes

Date:
2014-01-01

Citation:
Lau, C. L., Kovacevic, M., Tingleff, T. S., Forsythe, J. S., Cate, H. S., Merlo, D., Cederfur, C., Maclean, F. L., Parish, C. L., Horne, M. K., Nisbet, D. R. & Beart, P. M. (2014). 3D Electrospun scaffolds promote a cytotrophic phenotype of cultured primary astrocytes. Journal of Neurochemistry, 130 (2), pp.215-226. https://doi.org/10.1111/jnc.12702.

Persistent Link:
https://hdl.handle.net/11343/43807

Received Date : 14-Jan-2014

Revised Date : 24-Feb-2014

Accepted Date : 26-Feb-2014

Article type : Original Article

3D Electrospun scaffolds promote a cytotrophic phenotype of cultured primary astrocytes

Chew L. Lau[a,1], Michelle Kovacevic[a,1], Tine S. Tingleff[a,b], John S. Forsythe[c], Holly S. Cate[d], Daniel Merlo[a], Cecilia Cederfur[a], Francesca L. Maclean[e], Clare L. Parish[a], Malcolm K. Horne[a], David R. Nisbet[c,e,1], Philip M. Beart[a,1*]

[a]Florey Institute of Neuroscience and Mental Health, The University of Melbourne, Parkville 3010, Australia;

[b]Faculty of Health and Medical Sciences, University of Copenhagen, Denmark;

[c] Department of Materials Engineering, Monash University, Clayton 3800, Australia;

[d]Centre for Neuroscience Research, Department of Anatomy and Neuroscience, The University of Melbourne, Parkville 3010, Australia;

[e] Research School of Engineering, The Australian National University, Canberra 0200, Australia;

[1] These authors contributed equally to this work

This article has been accepted for publication and undergone full peer review but has not been through the copyediting, typesetting, pagination and proofreading process which may lead to differences between this version and the Version of Record. Please cite this article as an 'Accepted Article', doi: 10.1111/jnc.12702

This article is protected by copyright. All rights reserved.

Accepted Article

*Corresponding author at: Florey Institute of Neuroscience and Mental Health, The University of Melbourne, Parkville, Victoria 3010, Australia.

Tel: +61 3 8344 7324

Fax: +61 3 9347 0446

Email address: philip.beart@florey.edu.au

Running title: Electrospun scaffolds and astrocytes phenotypes

Key Words: Astrocyte; Gene expression; Cell culture; Bioengineering; Astrogliosis; Cytotrophic phenotype;

Abstract

Astrocytes are a target for regenerative neurobiology because in brain injury their phenotype arbitrates brain integrity, neuronal death and subsequent repair and reconstruction. We explored the ability of 3D scaffolds to direct astrocytes into phenotypes with the potential to support neuronal survival. Poly-ε-caprolactone (PCL) scaffolds were electrospun with random and aligned fibre orientations on which murine astrocytes were sub-cultured and analysed at 4 and 12 *div*. Astrocytes survived, proliferated and migrated into scaffolds adopting 3D morphologies, mimicking *in vivo* stellated phenotypes. Cells on random PCL scaffolds grew as circular colonies extending processes deep within sub-micron fibres, whereas astrocytes on aligned scaffolds exhibited rectangular colonies with processes following the direction of fibre alignment but also penetrating the scaffold. Cell viability was maintained over 12 *div*, and cytochemistry for F-/G-actin showed fewer stress fibres on bioscaffolds relative to 2D astrocytes. Reduced cytoskeletal

This article is protected by copyright. All rights reserved.

stress was confirmed by the decreased expression of glial fibrillary acidic protein (GFAP). PCR demonstrated up-regulation of genes (excitatory amino acid transporter 2, brain-derived neurotrophic factor and anti-oxidant) reflecting healthy biologies of mature astrocytes in our extended culture protocol. This study illustrates the therapeutic potential of bioengineering strategies using 3D electrospun scaffolds which direct astrocytes into phenotypes supporting brain repair.

Introduction

Repair of the injured central nervous system (CNS) requires reconstitution of neural networks through axon extension and synapse formation. Synapses in the CNS are in close apposition with astrocytes, which are recognised as plastic cells playing key roles in maintaining brain function via energetics, antioxidant activity, trophic factor synthesis, neurovascular coupling and L-glutamate (Glu) homeostasis (Ridet *et al.* 1997; Maragakis and Rothstein 2006; Parpura *et al.* 2012). Astrocytic morphological change with plasticity would not be unexpected in a cell with a large cell body, an extensive and diverse arbor, tight junctions with other astrocytes and end-feet on the blood-brain-barrier and vasculature (McMillian *et al.* 1994; Ridet *et al.* 1997; Panickar and Norenberg 2005). Not surprisingly astrocytes exhibit various morphological and biochemical changes in response to changes in their milieu induced by physiological and pathological events. Such changes occur across a continuum of events, being influenced by the prevailing extracellular milieu in disease and trauma and by the extent of multiple factors, which appear able to cause both short- and long-term responses (Ridet *et al.* 1997; Maragakis and Rothstein 2006). Whilst the terms astrogliosis and reactive gliosis can be found in the literature, astrocytes are now considered to exist in a variety of phenotypes that have pro-survival ("cytotrophic") and

This article is protected by copyright. All rights reserved.

Accepted Article

destructive ("cytotoxic") components (McMillian *et al.* 1994; Panickar and Norenberg 2005; Sofroniew and Vinters 2010). These phenotypes have been found in both the normal brain and brains affected by neurological diseases and there is recent evidence that astrocytes can dynamically change phenotypic components, an attractive target to promote endogenous repair if they can be directed into a cytotrophic phenotype supportive of neuronal survival and axon regrowth. Thus changing the physical and molecular phenotype of astrocytes may facilitate neural repair mechanisms (Maragakis and Rothstein 2006; Sofroniew and Vinters 2010).

Work from our laboratory, initially focusing on excitatory amino acid transporters (EAATs), documented in conventional cultured astrocytes that morphological changes *in vitro* induce alterations in biology and gene expression (Zagami *et al.* 2009; Lau *et al.* 2010; Lau *et al.* 2011; Lau *et al.* 2012; Sheean *et al.* 2013. The actin cytoskeleton and Rho GTPases (Rho, Rac, Cdc42) are fundamental determinants of cellular motility and migration (Le Clainche and Carlier 2008; Mattila and Lappalainen 2008). We found treatment of astrocytes with inhibitors of Rho kinase produced stellated morphology, less actin stress fibres and a shift in the F-/G-actin ratio to a predominance of G-actin (Lau *et al.* 2011). Here analyses of the astrocytic transcriptome confirmed major alterations to genes of the extracellular matrix (ECM), with elevated expression of EAAT2, brain-derived neurotrophic factor (BDNF) and key anti-oxidant genes (Lau *et al.* 2012) – findings suggestive of shift to a cytotrophic phenotype. Tissue engineering is another strategy where the use of scaffolds provides cues for cellular organization, survival and function (Stevens *et al.* 2005; Teo *et al.* 2006) and in concert with materials science to manipulate surface chemistry, fibre alignment, diameter and interfibre spacing can morphologically replicate components of the ECM (Stevens *et al.* 2005; Teo *et al.* 2006). We found that the implantation of

This article is protected by copyright. All rights reserved.

Accepted Article

Accepted Article

3D electrospun poly(ε-caprolactone) (PCL) scaffolds produced a delayed astrocytic response in the striatum in a rat model of traumatic brain injury (Nisbet *et al.* 2009). After 60 days, astrocyte numbers had returned to normal levels, but more importantly the PCL scaffold failed to elicit a prolonged foreign body reaction. Interestingly, neurites infiltrated into the randomly aligned scaffold during the peak in astrocytes activation, suggesting the infiltration was being promoted by astrocytes. This result led to our hypothesis that electrospun scaffolds may promote cytotrophic astrocytic phenotype. Here we have taken this postulate to a comparison *in vitro* of astrocytes cultured on electrospun 3D scaffolds and in conventional 2D mode. Investigations of astrocytic morphology and distribution on 3D electrospun scaffolds, as well as their ability to support cell survival, proliferation and functional outcomes of growth, demonstrated cellular penetration of astrocytic processes into the scaffolds and promotion of a cytotrophic phenotype; two key outcomes likely supportive of brain repair. Our evidence demonstrates that bioengineering astrocytes has great potential for regenerative neurobiology. A preliminary account of these findings was presented at the 43rd Meeting of the American Society for Neurochemistry (Beart *et al.* 2012).

Materials and Methods

All experimentation was approved by the Ethics Committee of the Florey Institute for Neuroscience and Mental Health and was undertaken according to the guidelines of the National Health and Medical Research Council (NHMRC, Australia).

Preparation of poly(ε-caprolactone) scaffolds

Poly(ε-caprolactone) PCL was obtained from Sigma Aldrich (St Louis, MO, USA, molecular weight 70,000 – 90,000). 2D PCL films were fabricated using a compression moulder heated to

This article is protected by copyright. All rights reserved.

80 °C. The PCL was held between two polished stainless steel plates covered with Teflon release film and allowed to reach temperature for 2 min. A 20 kPa force was then applied to the plates for 5 mins to fabricate the films before they were removed and quenched in an ice-water slurry. 3D electrospun scaffolds were fabricated as described previously (Nisbet *et al.* 2008) with minor modifications. Polymer solutions of 10% (w/v) were prepared for electrospinning by dissolving PCL in 2 ml of chloroform (Merck Pty Ltd., Australia) and methanol (Merck Pty Ltd., Australia) at a ratio of 3:1 (v/v). The solutions were placed into a glass syringe (10 ml) with a 21-gauge needle for electrospinning at a flow rate of 1.5 ml/hr. A 15 kV accelerating voltage was used at the positive electrode, with a ground rotating mandrel (diameter = 5cm) employed as the collector. The working distance was 18 cm and the collector was coated with aluminum foil for easy removal. Speeds of 200 rpm were used to fabricate randomly oriented fibres and 4,000 rpm to fabricate aligned fibres. Once removed from the collector, PCL scaffolds where then cut into circles using a punch with diameters matching the dimensions of the wells (96- and 24-well plates). The scaffolds were sterilised in 70% ethanol for 15 min and washed with sterilised phosphate buffered saline (PBS) pH 7.4 prior to use.

Scaffold characterisation

The morphology of the scaffolds was characterised using scanning electron microscopy (SEM). The samples were sputter coated with platinum at 20 mA for 1 minute. All SEM images were taken under 3 kV with a working distance of 3.5 mm on a Zeiss UltraPlus FESEM. The average diameters of the fibres were determined using Image J to measure a total of 20 fibres across four different samples and were 400 ± 110 and 450 ± 150 nm, for random and aligned scaffolds, respectively (Figure 1).

This article is protected by copyright. All rights reserved.

Accepted Article

Accepted Article

Cell Culture

All media used for primary cell culture and maintenance were from Gibco®, Life Technologies (Melbourne, Australia) unless otherwise stated. Primary cultures of astrocytes were established from the forebrain of postnatal day 1.5 C57 Black 6 mice (animal facilities of Florey Institute for Neuroscience and Mental Health) as previously described (O'Shea *et al.* 2006). After astrocytes had formed a confluent layer (10 *div*), flasks were shaken overnight (to remove cells other than astrocytes) in a Ratek Orbital Mixer Incubator (180 rpm, 37 °C). Subculturing generated secondary cultures where astrocytes were seeded on to 24-well plates (polystyrene plate, glass coverslips or 2D PCL at 2×10^4 cells/well) or 96-well plates (polystyrene plate, random or aligned 3D PCL at 8×10^3 cells/well) depending on the experiment, and incubated in a humidified incubator at 37 °C with 5% CO_2. Scaffolds were held at the bottom of the well by sterile glass inserts. Preliminary experiments explored the optimal cell density, examining seeding densities of 4, 8 and 16×10^3 cells/well (Supplementary Figure 1). A full medium change was performed to remove non-adherent cells and medium was subsequently changed every 3–4 days until cells were ready for use (4 *div* or 12 *div* following subculturing). Immunocytochemistry with glial fibrillary acidic protein (GFAP) revealed the presence of a monolayer of astrocytes (Apricò *et al*. 2004; O'Shea *et al.* 2006). Note: 4 *div* and 12 *div* following subculturing is equivalent to 14 *div* and 22 *div* but for simplicity will be referred to in this paper as 4 *div* and 12 *div*.

Immunocytochemistry

The immunocytochemical procedures have been described previously (Lau *et al.* 2011). Astrocytes grown on glass coverslips, 2D PCL films, aligned or random scaffolds were fixed in 4% paraformaldehyde in PBS for 10 min. Cells were incubated with primary antibodies GFAP

This article is protected by copyright. All rights reserved.

(1:1000, Chemicon International Inc, Melbourne, Australia) at 4 °C overnight, followed by secondary antibody (Alexa Fluor® 488, Molecular Probes® Life Technologies, Melbourne, Australia) incubation for 3 h at room temperature. Coverslips and scaffolds were mounted on glass microscope slides with DAKO fluorescence mounting medium (DAKO, Victoria, Australia), left to dry in the dark overnight and stored at 4 °C. Fluorescence was visualised under an Olympus IX71 inverted microscope (Olympus Australia Pty Ltd, Melbourne, Japan). Digital images were acquired using an Olympus Camedia C-5050 Zoom digital camera attached to the Olympus IX71 inverted microscope.

Cytoskeletal staining

As described previously (Lau *et al.* 2011), concurrent labelling of F- and G-actin was obtained by staining with TRITC-conjugated phalloidin (1:1000, Sigma Aldrich, Melbourne, Australia) and Alexa Fluor® 488-conjugated deoxyribonuclease I (DNaseI, 1:250; Molecular Probes® Life Technologies), respectively.

Confocal imaging

Astrocytes were prepared on scaffolds and immunoreacted with GFAP (see above). Nuclei were stained using Hoechst 33342 (5 μg/ml; Molecular Probes® Life Technologies) and the fluorescence was visualised under Leica SP8 Confocal Microscope (Leica Microsystems, Wetzlar, Germany). The scaffolds were imaged using reflection of a HeNe 633 nm laser. Z-stacks were obtained with optical sectioning at 0.2 μm.

This article is protected by copyright. All rights reserved.

Accepted Article

Cell viability and function assays

Cellular viability was assessed using a MTT (3-(4,5-dimethylthiazol-2-yl)-2,5-diphenyltetrazolium bromide) reduction assay according to the manufacturer's instructions (Lau *et al.* 2011). Additionally a lactate dehydrogenase (LDH) assay was carried out using a Cytotoxicity Detection Kit (Roche, Sydney, Australia) according to the manufacturer's instructions (Lau *et al.* 2011).

L-Glutamate uptake: Activity of astrocytic excitatory amino acid transporters (EAATs) was determined using [^{3}H]-D-aspartate ([^{3}H]-D-Asp) uptake (Apricò *et al*. 2004). In brief, cells were pre-incubated at 37 °C for 5 min and then incubated with [^{3}H]-D-Asp (50 nM, 5 min), with or without the unlabelled D-Asp (1 mM) in uptake buffer (135 mM NaCl, 5 mM KCl, 0.6 mM $MgSO_4$, 1 mM $CaCl_2$, 6 mM D-glucose, 10 mM HEPES, pH 7.5). Uptake was terminated by washing at 4 °C, and accumulated radioactivity determined by scintillation spectrometry (O'Shea *et al.* 2006).

Western blot analysis

As described previously (Lau *et al.* 2010), cells were grown in polystyrene micro-well plates, with or without aligned and random PCL scaffolds for 12 *div*. Samples were pooled from eight wells (n = 8 replicates), and total cell protein concentration was determined with the Bio-Rad Dc Assay Kit (Sydney, Australia) according to the manufacturer's instructions. Standard Western blot protocols were carried out with 10 µg protein per lane (three lanes per condition, where each lane represents an independent experiment) and membranes were incubated with primary GFAP antibodies at 1:1000 (Promega, Melbourne, Australia) overnight at 4 °C. Following washing, membranes were incubated with horseradish-peroxidase conjugated secondary antibodies (goat

This article is protected by copyright. All rights reserved.

Accepted Article

anti-rabbit IgG, 1:1000) for 3 h at room temperature. Proteins were then visualised using enhanced chemiluminescence. As a control for protein loading, blots were subsequently probed for β-actin (primary antibody 1:10000) using the same procedures. Densitometric analysis of Western blots was performed using ImageJ software (http://rsb.info.nih.gov.ij/ National Institutes of Health, Bethesda, MD, USA, version 1.46r) to measure the area and density of proteins bands after subtracting the background of the autoradiographic film (Cimarosti *et al.* 2005).

Quantitative real-time PCR (qRT-PCR)

RNA was extracted from astrocytes grown on polystyrene micro-well plates, 2D PCL, aligned and random electrospun scaffolds. Total RNA was extracted from four independent cultures with eight replicates per culture using the RNeasy Mini Kit (Qiagen, Alameda, CA) according to the manufacturer's instructions. In order to quantify the RNA extract, 1.8µl of RNA sample was used for spectrophotometric analysis using NanoDrop ND-1000 (NanaDrop Technologies, Inc., Wilmington, DE). qRT-PCR was performed on an ViiA 7 sequence detection system (Applied Biosystems, Foster City, CA) as previously described (Binder *et al.* 2008). Primers were designed using Primer Express 3.0 (Applied Biosystems, Melbourne, Australia). Sequences of primers and details of all procedures were published previously (Lau *et al.* 2012). To determine statistical significance for qRT-PCR data, 95% confidence intervals were constructed for single-variable analysis. All data are presented as mean ± SEM, and are expressed relative to the control condition (polystyrene or 2D PCL).

This article is protected by copyright. All rights reserved.

Accepted Article

Accepted Article

Data analysis

Specific details are given above. All values are mean ± SEM from replicate determinations from multiple independent experiments. Data were subjected to one-way analysis of variance (ANOVA) followed by Dunnett's Multiple Comparison *post-hoc* Test using GraphPad Prism v.4.0 (GraphPad, San Diego, CA, USA).

Results

Dramatic change in astrocytic morphology on 3D PCL

Initial work explored optimal culture conditions by investigating GFAP immunolabelling and observations based upon length of GFAP-positive astrocytic processes and indicated a density of 8×10^3 cells/well yielded viable cultures (Supplementary Figure 1). Under these conditions, astrocytes grown under control conditions on coverslips were evenly distributed at 4 *div* and appeared as flattened cells (Figure 2A), with increased cell number at 12 *div* (Figure 2B). When cultured on random scaffolds, astrocytes appeared as tight colonies (ratio of larger to smaller axis < 2) at 4 *div* (Figure 2), and these colonies expanded to occupy the scaffold with condensed processes (typically 50-75 µm) by 12 *div*. By comparison, astrocytes grown on aligned scaffolds grew in colonies that were more rectangular (ratio of larger to smaller axis ≥ 2) (Figure 2E at 4 *div*) than those growing on random scaffolds (Figure 2C), with processes aligning with the fibres and by 12 *div* extending for lengths sometimes exceeding 300 µm (Figure 2F). Morphological estimates of the length of GFAP-positive processes at 12 *div* were 65 ± 3 µm and 90 ± 3 µm (≥ 15 images, 3 independent experiments) for random and aligned scaffolds, respectively.

As actin is central to cellular morphology and plays a key role in regulating cellular responses to the extracellular matrix (Provenzano and Keely 2011), its arrangement on the 3D scaffolds was

This article is protected by copyright. All rights reserved.

studied by staining astrocytes for its two forms, filamentous, F-actin, and globular, G-actin (Figure 3). The intensity of G- and F- actin staining on 3D scaffolds was higher than on coverslips (2D). Furthermore, by 12 *div* F-actin staining in 2D was uniformly cobblestoned reflecting astrocyte morphology (Figure 3A, C), whereas G-actin staining was barely detectable at both 4 *div* and 12 *div* (Figure 3B, D), but was consistently expressed on both 3D scaffolds at both time points (Figure 3F, H, J, L). The organization of F- and G-actin stained colonies on random and aligned scaffolds reflected the pattern discerned by GFAP immunohistochemistry (Figure 2).

Astrocytes on 3D scaffolds maintain viability but show decreased total protein and GFAP levels at 12 div

Prolonged culturing of astrocytes under control conditions and on aligned PCL scaffolds resulted in a significant reduction in mitochondrial function (Figure 4A). Reduction in mitochondrial function, as shown by MTT activities, was similar at 12 *div* regardless of the culture conditions. In addition, nuclear condensation and fragmentation were not observed at 12 *div,* consistent with the absence of pyknotic nuclei (See Supplementary Figure 2). LDH, an extracellular measure of compromised cell membrane, was significantly higher in astrocytes grown on polystyrene (control) and aligned scaffolds at 4 *div* than in those cultured till 12 *div* ($p < 0.05$). Surprisingly, the LDH of cells grown on aligned scaffolds was higher than those grown on polystyrene (control, $p < 0.05$) (Figure 4B). Total cellular protein increased between 4 *div* and 12 *div*, regardless of the surface on which cells were cultured and was taken as an indication of astrocytic proliferation within the eight days (Figure 4C). However, cellular protein concentration of astrocytes grown on the 3D scaffolds was significantly lower (~30-40%

This article is protected by copyright. All rights reserved.

Accepted Article

decreases at 12 *div)* than those grown on polystyrene (random $p < 0.001$ and aligned $p < 0.05$) at 12 *div*. [^{3}H]-D-Asp uptake activity, which is an index of Glu transport and thus reflects astrocytic function (Beart and O'Shea 2007), was similar in all culture conditions. On the basis of the studies described above, 12 *div* was chosen as the timepoint for further investigation.

Western immunoblotting studies were undertaken for GFAP (Figure 5), a main constituent of intermediate filaments in astrocytes, and an index classically increased in reactive astrocytes (Middeldorp and Hol 2011). The expression of GFAP in astrocytes grown on both random and aligned scaffolds decreased appreciably (~80% reductions) relative to those maintained in 2D culture at 12 *div* (polystyrene, $p < 0.01$).

Astrocytic interaction with the 3D scaffolds

Confocal imaging indicated that GFAP-positive fibres penetrated into the fibre network of aligned and random PCL scaffolds (Figure 6A and 6B respectively). Image analysis allowed the concurrent visualisation of GFAP-positive fibres and digital sectioning demonstrated that processes extended up to 10 µm into the scaffolds, including projecting to the base of the scaffolds (Figure 6). Hoechst-labelled nuclei were also visualised within the 3D PCL, indicating that astrocytes were capable of migrating deep into the scaffolds. Astrocytes appeared not to show any obvious preference with respect to their capacities to penetrate into random or aligned scaffolds.

Gene expression

Given the extensive changes in astrocytic morphology and GFAP expression, we sought molecular insights into genes that might contribute to the transformation of phenotype. Our

This article is protected by copyright. All rights reserved.

Accepted Article

previous study (Lau *et al.* 2012) focused attention on select genes involved in: i) cell motility and pathfinding (ACTA2, VCL, CXCL12), ii) TGFβ-related migration (TAGLN), iii) astrocytic function, including Glu transport (SLC1A2 = EAAT2), BDNF and anti-oxidant (GSTA1 and HMOX1) activities. The mRNA expression of all of these genes was significantly greater in astrocytes cultured on the 3D scaffolds, regardless of their fibre alignment (Figure 7), relative to conventional 2D cultures. PCL itself possessed properties that induced increased mRNA expression, since expression of ACTA2, VCL, CXCL12 and BDNF were increased in astrocytes grown on either 2D and 3D PCL (both random and aligned) scaffolds (Figure 7). mRNA expression of TAGLN, a gene linked to transforming growth factor ß–mediated cellular migration, in astrocytes grown on 3D aligned scaffolds was significantly greater than astrocytes grown on control scaffolds and 2D PCL film, suggesting this increase is due to the 3D morphology and topography of the PCL scaffold (Figure 7). Similar increases in mRNA expression of the major Glu transporter SLC1A2 and GSTA1, a key enzyme for glutathione synthesis, in conjunction with the BDNF data, suggest that the electrospun fibres had promoted a salutary astrocytic phenotype.

Discussion

Astrocytes offer great potential for regenerative neurobiology because of the fundamental roles they play in the function of the CNS, participating in many physiological events including synaptic transmission, maintenance of neurotransmitter homeostasis, cerebral blood flow and as a site of anti-oxidant defence during stress. Astrocytic responses occur as a continuum that is graded according to the extent of the trauma or disease - when minor there is resolution and even the extreme scenario of glial scar formation is considered manageable by pharmacological

This article is protected by copyright. All rights reserved.

Accepted Article

intervention (Ridet *et al.* 1997; Mueller *et al.* 2009; Sofroniew 2009). Our interest in taking advantage of the biology of astrocytes to promote repair and regeneration was driven by our documentation of phenotypes *in vitro* (Lau *et al.* 2012) and *in vivo* (Nisbet *et al.* 2009) consistent with a pro-survival state. In these studies different interventions resulted in cytotrophic properties that potentially could result in beneficial outcomes. Here we have used engineered scaffolds to influence astrocytic phenotype with the ultimate goal of understanding how the inflammatory cascade might be tuned to generate a favourable outcome. Key findings emergent from our study were that astrocytes survived and migrated on 3D PCL scaffolds with a stellated morphology, adopting a phenotype where the reduced pattern of GFAP expression and overall gene profile were likely to be cytotrophic in a reactive milieu.

Cell morphology and behaviour

When astrocytes were cultured on the 3D scaffolds, they initially formed colonies with condensed processes and then adopted elongated and ramified cell morphologies. Given the relative increase in G-actin staining (i.e. fewer stress fibres) and an ~80% decrease in GFAP expression, our data indicate these cells are less stressed compared to cells grown in the conventional 2D culture system. The morphology of the cells changed dramatically as they extended processes over the substratum to occupy vacant space. This cytoskeletal event is considered an important determinant of cell growth and survival (O'Neill *et al.* 1986; Schnell *et al.* 2007; Horne *et al.* 2010). At 12 *div* we demonstrated that the survival and viability of astrocytes grown on the 3D PCL scaffolds was maintained with findings suggestive of adoption of a quiescent state after the initial proliferation and expansion (c.f. Figure 4). While cellular proliferation was supported by 3D scaffolds, the large reduction in GFAP levels relative to only a

This article is protected by copyright. All rights reserved.

Accepted Article

~30-40% decrease in total protein is indicative of a genuine shift in astrocytic phenotype on PCL scaffolds.

Given the tendency for astrocytes to form colonies as early as 4 *div* on the scaffolds, contact inhibition (or density-dependent inhibition of cell division) may be occurring in these conditions (Martz and Steinberg 1972). However, nutrient supply is thought to be more important than the effects of cell-cell contact, so the pattern of organization of high-density cultures may be a contributing factor to their slower rate of cell proliferation. Thus cellular density and the reduced nutrient supply, as well as the toxic build-up of waste products, likely influenced viability at the density of 16×10^3 cells/well (Owen and Shoichet 2010), where there were extensive overlapping layers of astrocytes. Moreover, for both types of 3D scaffolds GFAP-positive processes were significantly longer at the 8×10^3 relative to 4×10^3 cells/well at 12 *div* (Supplementary Figure 2), suggesting this density was optimal in terms of cell-cell contact required for astrocytic growth. Density-dependent inhibition of cell division may help explain the reduction in glial scarring observed in rat striatum when treated with PCL scaffolds *in vivo* (Nisbet *et al.* 2009), considering astrocyte proliferation soon after injury has been associated with a destructive phenotype (Parish *et al.* 2002).

Cell-scaffold interactions: cytoskeletal evidence for increased cellular migration

Electrospun scaffolds are engineered to mimic the native ECM, and both the fibre orientation and topography have a profound affect astrocytic shape, growth and function (Gerardo-Nava *et al.* 2009; Singhvi *et al.* 1994). The present results demonstrate that aligned scaffolds provide contact guidance cues that allow for longer and more directed process outgrowth (Z-stack, Figure 6) even though migration and penetration of cell bodies into both random and aligned scaffolds

This article is protected by copyright. All rights reserved.

Accepted Article

Accepted Article

was similar. This ability of electrospun scaffolds to influence the behaviour and directionality of astrocytic growth is thus of particular interest to CNS repair strategies attempting to target specific areas of injury and direct the outgrowth of regenerating axons (East *et al.* 2010) Astrocytes have been grown successfully on micro-grooved and -patterned substrates (Sorensen *et al.* 2007; Meng *et al.* 2012) but these topographies do not offer the 3D advantages of our scaffolds. Attempts to culture astrocytes on electrospun fibres have generally been hampered by issues related to poor proliferation and cytoskeletal stress (Cao *et al.* 2012; Kim *et al.* 2012), and our success shows the advantages of employing secondary cultures of astrocytes in combination with electrospun scaffolds. When this study was essentially complete the successful maintenance of astrocytes in 3D was reported on electrospun scaffolds (Puschmann *et al.* 2013; Zuidema *et al.* 2014). Our procedure has the important advantage over both these studies that it allows 3D culture over an extended time interval of more mature astrocytes under conditions where there is preservation of the cytotrophic phenotype with an extensively arborized cellular architecture featuring numerous major and minor processes.

Normally astrocytes are grown *in vitro* as a 2D monolayer, which is very different to their 3D environment *in vivo*. Unlike the recent work by Zuidema *et al*. (2014), who undertook extensive characterization of astrocytic architecture in 2D, we used confocal Z-stacks in conjunction with Hoechst staining, and cytochemistry for GFAP to demonstrate that cells migrate and penetrate through the scaffold from its top through its middle to the base. The mean fiber diameter of our electrospun fibers was appreciably less (0.4 versus 2 μm) than that of Zuidema *et al*. (2014), who also employed fibronectin, conditions that are likely to encourage adhesion and extensive growth and migration (Wang *et al*. 2009) along their scaffolds. Importantly, the appreciable penetration

This article is protected by copyright. All rights reserved.

of astrocytes processes into our biomatrices achieved one of the key aim of our study to produce 3D astrocytes. Interestingly, both scaffolds lead to promotion of Glu transport, but guided by our earlier evidence for cytoskeletal changes (Lau *et al*. 2012) we also demonstrated reduced expression of GFAP and actin stress fibers in conjunction with upregulation of BDNF and anti-oxidant genes. These data suggest that the current difficulty in correlating healthy, stellated *in vivo* astrocytic phenotypes with flat, cobblestone-like morphologies displayed *in vitro* may be overcome by using electrospun 3D scaffolds as a substrate to induce more physiologically representative astrocytes for *in vitro* studies of cellular behaviour and morphology.

Cellular interaction with different substrates can activate different cellular and ECM mechanisms linked to the control of astrocytic cytoskeletal arrangement (Provenzano and Keely 2011). The actin cytoskeleton has been well established to have important roles in cell morphology and migration, with astrocytic process formation occurring due to depolymerization of actin filaments via a shift from F-actin to G-actin (Kimelberg 2004; Lau *et al.* 2011). This study found that control cultures of primary astrocytes have a high F- to G-actin ratio and numerous focal adhesions. Increases in both F- and G- actin observed in astrocytes cultured on random and aligned fibres are most likely a reflection of process elongation on these scaffolds. These data suggest that control cells are at higher levels of cytoskeletal stress, possibly due to the non-compliant 2D substrate (glass/polystyrene) on which they were seeded, whereas PCL scaffolds more clearly reflect the elastic modulus encountered *in vivo*. This interpretation is also supported by our immunoblotting data of GFAP expression, which was decreased in astrocytes grown on both random and aligned scaffolds rather than upregulated as would occur in inflammatory response occurring in CNS insults (Middeldorp and Hol 2011).

This article is protected by copyright. All rights reserved.

Accepted Article

The pathways that regulate actin polymerization are not fully characterised, however the GTPases (Rho, Rac and Cdc42) are known be involved (Goldman and Abramson 1990; Hall 1998; Etienne-Manneville and Hall 2002). Extensive work in our laboratory has shown that following treatment with the Rho kinase inhibitors, cultures of murine astrocytes shift from a flat, cobblestone phenotype to a stellate shape, with a concomitant decrease in F-actin and a proportional increase in G-actin (Lau *et al*. 2011) and adoption of a cytotrophic phenotype (Lau *et al*. 2012). Astrocytes grown on the PCL scaffolds showed similar increases in "healthy" genes, especially the SLC1A2 (i.e. EAAT2) and antioxidant-linked GSTA1, indicating that 3D scaffolds promote a transition to a cytotrophic phenotype. Our observation of increased SLC1A2 is consistent with Zuidema *et al*. (2014), who also found EAAT1 expression was elevated on their bioscaffold. Expression of the neurotrophin BDNF was always elevated on PCL, including on both random and aligned scaffolds. Indeed, there is evidence that SLC1A2 and BDNF may be co-regulated in health and pathology (Gourley et al. 2012; Lau et al. 2012; Xu et al. 2008). The up-regulation of SLC1A2 expression found on the scaffolds was also found with ROCK inhibitors (Lau *et al*. 2012) and likely represents the homeostatic behavior displayed by astrocytes to maintain this key transporter (Abe and Misawa 2003; Zagami *et al.* 2009; Lau *et al*. 2010) integral to the CNS defence against excitotoxicity. Key indices of the healthy phenotype would appear to be not only elevated expression of SLC1A2, but also of the major antioxidant gene, GSTA1, together with decreased GFAP and an accompanying increase in G-actin.

Conclusion

These results show that astrocytes cultured on electrospun 3D PCL scaffolds have extended processes that penetrate the scaffold. Importantly, decreased expression of the astrocytic

This article is protected by copyright. All rights reserved.

Accepted Article

intermediate filament marker GFAP and increased G-actin suggested astrocytes adopted biologies that were less stressed, whilst displaying elevated expression of genes indicative of a cytotrophic phenotype. This study points to the therapeutic potential of bioengineering strategies using 3D electrospun scaffolds of differing fibre orientations that direct astrocytes into phenotypes supporting brain repair.

Acknowledgements

The authors would like to thank Ms Alexandra Rodriguez and Kiara Bruggeman for critical reading of the manuscript. This research was supported by funding from an NHMRC project grant (APP1020332). DRN was supported by an Australian Research Council Australian Postdoctoral Fellowship and subsequently by an NHMRC Career Development Fellowship (APP1050684). MKH and PMB were supported NHMRC Research Fellowships, APP1020401 and APP1019833, respectively. CLP is a Senior Medical Research Fellow supported by the Viertel Charitable Foundation, Australia. Access to the facilities of the Centre for Advanced Microscopy (CAM) with funding through the Australian Microscopy and Microanalysis Research Facility (AMMRF) is gratefully acknowledged.

References

Abe K andMisawa M (2003). Astrocyte stellation induced by Rho kinase inhibitors in culture. *Brain Res Dev Brain Res* 143:99-104.

Apricò K, Beart PM, Crawford D and O'Shea RD (2004). Binding and transport of [3H](2S,4R)-4-methylglutamate, a new ligand for glutamate transporters, demonstrate labeling of EAAT1 in cultured murine astrocytes. *J Neurosci Res* 75:751-9.

This article is protected by copyright. All rights reserved.

Accepted Article

Accepted Article

Beart PM and O'Shea RD (2007). Transporters for L-glutamate: an update on their molecular pharmacology and pathological involvement. *Br J Pharmacol* 150:5-17.

Beart PM, Kovacevic M, Lau CL, Horne MK, Forsythe JS and Nisbet DR (2012). Astrocytes maintained on 3D nanofibrous scaffolds exhibit healthy morphologies appropriate for regenerative neurobiology: In: Rasband M, editor: Transactions of the American Society for Neurochemistry for 43rd ASN Annual Meeting; March 3-7; Baltimore, USA: 2012. p. 101.

Binder MD, Cate HS, Prieto AL, Kemper D, Butzkueven H, Gresle MM, Cipriani T, Jokubaitis VG, Carmeliet P and Kilpatrick TJ (2008). Gas6 deficiency increases oligodendrocyte loss and microglial activation in response to cuprizone-induced demyelination. *J Neurosci* 28:5195-206.

Cao H, Marcy G, Goh EL, Wang F, Wang J and Chew SY (2012). The effects of nanofiber topography on astrocyte behavior and gene silencing efficiency. *Macromol Biosci* 12:666-74.

Cimarosti H, Jones NM, O'Shea RD, Pow DV, Salbego C and Beart PM (2005). Hypoxic preconditioning in neonatal rat brain involves regulation of excitatory amino acid transporter 2 and estrogen receptor alpha. *Neurosci Lett* 385:52-7.

East E, de Oliveira DB, Golding JP and Phillips JB (2010). Alignment of astrocytes increases neuronal growth in three-dimensional collagen gels and is maintained following plastic compression to form a spinal cord repair conduit. *Tissue Eng Part A* 16:3173-84.

Etienne-Manneville S, Hall A. Rho GTPases in cell biology. Nature 2002;420:629-35.

Gerardo-Nava J, Führmann T, Klinkhammer K, Seiler N, Mey J, Klee D, Möller M, Dalton PD and Brook GA (2009). Human neural cell interactions with orientated electrospun nanofibers in vitro. *Nanomedicine (Lond)* 4:11-30.

Goldman JE and Abramson B (1990). Cyclic AMP-induced shape changes of astrocytes are accompanied by rapid depolymerization of actin. *Brain Res* 528:189-96.

This article is protected by copyright. All rights reserved.

Accepted Article

Gourley SL, Espitia JW, Sanacora G and Taylor JR (2012). Antidepressant-like properties of oral riluzole and utility of incentive disengagement models of depression in mice. *Psychopharmacology (Berl)* 219:805-14.

Hall A (1998). Rho GTPases and the actin cytoskeleton. *Science* 279:509-14.

Horne MK, Nisbet DR, Forsythe JS and Parish CL (2010). Three-dimensional nanofibrous scaffolds incorporating immobilized BDNF promote proliferation and differentiation of cortical neural stem cells. *Stem Cells Dev* 19:843-52.

Kimelberg HK (2004). The problem of astrocyte identity. *Neurochem Int* 45:191-202.

Kim SH, Shin C, Min SK, Jung SM and Shin HS (2012). In vitro evaluation of the effects of electrospun PCL nanofiber mats containing the microalgae Spirulina (Arthrospira) extract on primary astrocytes. *Colloids Surf B Biointerfaces* 90:113-8.

Lau CL, Beart PM and O'Shea RD (2010). Transportable and non-transportable inhibitors of L-glutamate uptake produce astrocytic stellation and increase EAAT2 cell surface expression. *Neurochem Res* 35:735-42.

Lau CL, O'Shea RD, Broberg BV, Bischof L and Beart PM (2011). The Rho kinase inhibitor Fasudil up-regulates astrocytic glutamate transport subsequent to actin remodelling in murine cultured astrocytes. *Br J Pharmacol* 163:533-45.

Lau CL, Perreau VM, Chen MJ, Cate HS, Merlo D, Cheung NS, O'Shea RD and Beart PM (2012). Transcriptomic profiling of astrocytes treated with the Rho kinase inhibitor fasudil reveals cytoskeletal and pro-survival responses. *J Cell Physiol* 227:1199-211.

Le Clainche C and Carlier MF (2008). Regulation of actin assembly associated with protrusion and adhesion in cell migration. Physiol Rev 88:489-513.

This article is protected by copyright. All rights reserved.

Accepted Article

Maragakis NJ and Rothstein JD (2006). Mechanisms of disease: astrocytes in neurodegenerative disease. *Nat Clin Pract Neurol* 2:679-89.

Martz E and Steinberg MS (1972). The role of cell-cell contact in "contact" inhibition of cell division: a review and new evidence. *J Cell Physiol* 79:189-210.

Mattila PK and Lappalainen P (2008). Filopodia: molecular architecture and cellular functions. Nat Rev Mol Cell Biol 9:446-54.

McMillian MK, Thai L, Hong KS, O'Callaghan JP and Pennypacker KR (1994). Brain injury in a dish: a model for reactive gliosis. *Trends Neurosci* 17:138-42.

Meng F, Hlady V and Tresco PA (2012). Inducing alignment in astrocyte tissue constructs by surface ligands patterned on biomaterials. *Biomaterials* 33:1323-35.

Middeldorp J and Hol EM (2011). GFAP in health and disease. *Prog Neurobiol* 93:421-43.

Mueller BK, Mueller R and Schoemaker H (2009). Stimulating neuroregeneration as a therapeutic drug approach for traumatic brain injury. *Br J Pharmacol* 157:675-85.

Nisbet DR, Yu LM, Zahir T, Forsythe JS and Shoichet MS (2008). Characterization of neural stem cells on electrospun poly(epsilon-caprolactone) submicron scaffolds: evaluating their potential in neural tissue engineering. *J Biomater Sci Polym Ed* 19:623-34.

Nisbet DR, Rodda AE, Horne MK, Forsythe JS andFinkelstein DI (2009). Neurite infiltration and cellular response to electrospun polycaprolactone scaffolds implanted into the brain. *Biomaterials* 30:4573-80.

O'Neill C, Jordan P and Ireland G (1986). Evidence for two distinct mechanisms of anchorage stimulation in freshly explanted and 3T3 Swiss mouse fibroblasts. *Cell* 44:489-96.

O'Shea RD, Lau CL, Farso MC, Diwakarla S, Zagami CJ, Svendsen BB, Feeney SJ, Callaway JK, Jones NM, Pow DV, Danbolt NC, Jarrott B and Beart PM (2006). Effects of

This article is protected by copyright. All rights reserved.

lipopolysaccharide on glial phenotype and activity of glutamate transporters: Evidence for delayed up-regulation and redistribution of GLT-1. *Neurochem Int* 48:604-10.

Owen SC and Shoichet MS (2010). Design of three-dimensional biomimetic scaffolds. *J Biomed Mater Res A* 94:1321-31.

Panickar KS and Norenberg MD (2005). Astrocytes in cerebral ischemic injury: morphological and general considerations. *Glia* 50:287-98.

Parish CL, Finkelstein DI, Tripanichkul W, Satoskar AR, Drago J and Horne MK (2002). The role of interleukin-1, interleukin-6, and glia in inducing growth of neuronal terminal arbors in mice. *J Neurosci* 22:8034-41.

Parpura V., Heneka M.T., Montana V., Oliet S.H.R., Schousboe A., Haydon, P.G., Stout Jr R.F., Spray D.C., Reichenbach A., Pannicke T., Pekny M., Pekna M., Zorec R. and Verkhratsky A. (2012). Glial cells in (patho)physiology. *J Neurochem* 121:4-27

Puschmann TB, Zandén C, De Pablo Y, Kirchhoff F, Pekna M, Liu J and Pekny M (2013). Bioactive 3D cell culture system minimizes cellular stress and maintains the *in vivo*-like morphological complexity of astroglial cells. *Glia* 61:432-40.

Provenzano PP and Keely PJ (2011). Mechanical signaling through the cytoskeleton regulates cell proliferation by coordinated focal adhesion and Rho GTPase signaling. *J Cell Sci* 124:1195-205.

Ridet JL, Malhotra SK, Privat A and Gage FH (1997). Reactive astrocytes: cellular and molecular cues to biological function. *Trends Neurosci* 20:570-77.

Schnell E, Klinkhammer K, Balzer S, Brook G, Klee D, Dalton P and Mey (2007) J. Guidance of glial cell migration and axonal growth on electrospun nanofibers of poly-epsilon-caprolactone and a collagen/poly-epsilon-caprolactone blend. *Biomaterials* 28:3012-25.

This article is protected by copyright. All rights reserved.

Accepted Article

Accepted Article

Sheean RK, Lau CL, Shin YS, O'Shea RD and Beart PM (2013). Links between l-glutamate transporters, Na(+)/K(+)-ATPase and cytoskeleton in astrocytes: evidence following inhibition with rottlerin. *Neuroscience* 254:335-46.

Singhvi R, Kumar A, Lopez GP, Stephanopoulos GN, Wang DI, Whitesides GM and Ingber DE (1994). Engineering cell shape and function. *Science* 264:696-8.

Sofroniew MV (2009). Molecular dissection of reactive astrogliosis and glial scar formation. *Trends Neurosci* 32:638-47.

Sofroniew MV and Vinters HV (2010). Astrocytes: biology and pathology. *Acta Neuropathol* 119:7-35.

Sorensen A, Alekseeva T, Katechia K, Robertson M, Riehle MO and Barnett SC (2007). Long-term neurite orientation on astrocyte monolayers aligned by microtopography. *Biomaterials* 28:5498-508.

Stevens MM, Mayer M, Anderson DG, Weibel DB, Whitesides GM and Langer R (2005). Direct patterning of mammalian cells onto porous tissue engineering substrates using agarose stamps. *Biomaterials* 26:7636-31.

Teo WE, He W and Ramakrishna S (2006). Electrospun scaffold tailored for tissue-specific extracellular matrix. *Biotechnol J* 9:918-29.

Wang XL, Yu T, Zhang JS, Yan QC and Luo YH (2009). Fibronectin and focal adhesion kinase small interfering RNA modulate rat retinal Müller cells adhesion and migration. *Cell Mol Neurobiol* 29:549-56.

Xu S, Han JC, Morales A, Menzie CM, Williams K and Fan YS (2008). Characterization of 11p14-p12 deletion in WAGR syndrome by array CGH for identifying genes contributing to mental retardation and autism. *Cytogenet Genome Res* 122:181-7.

This article is protected by copyright. All rights reserved.

Accepted Article

Zagami CJ, Beart PM, Wallis N, Nagley P and O'Shea RD (2009). Oxidative and excitotoxic insults exert differential effects on spinal motoneurons and astrocytic glutamate transporters: Implications for the role of astrogliosis in amyotrophic lateral sclerosis. *Glia* 57:119-35.

Zuidema JM, Hyzinski-García MC, Van Vlasselaer K, Zaccor NW, Plopper GE, Mongin AA and Gilbert RJ (2014). Enhanced GLT-1 mediated glutamate uptake and migration of primary astrocytes directed by fibronectin-coated electrospun poly-l-lactic acid fibers. *Biomaterials* 35:1439-49.

Figure legends:

Figure 1 SEM images of a (A) random and (B) aligned electrospun PCL scaffolds, with a mean diameter of 400 ± 110 nm and 450 ± 150 nm respectively. Scale bar = 1 μm

Figure 2 Temporal changes in astrocytic morphology on different matrices. Primary astrocytes were subcultured on coverslips (A, B), random PCL (C, D) and aligned PCL scaffolds (E, F) for 4 *div* (A, C, E) or 12 *div* (B, D, F) and stained for GFAP expression. Scale bar = 50 μm

Figure 3 Effects of days in culture and PCL scaffolds on F-/G-actin expression. Primary astrocytes were subcultured on coverslips (A, B, C, D), random PCL (E, F, G, H) and aligned PCL scaffolds (I, J, K, L) for 4 *div* (A, B, E, F, I, J) and 12 *div* (C, D, G, H, L, M) and stained for F-actin (TRITC-phalloidin; red) or G-actin (Alexa Fluor® 488-conjugated DNaseI; green). Scale bar = 100 μm

Figure 4 Comparison of temporal changes in cell viability (A, B), total protein (C) and EAAT activity (D) of astrocytes cultured on different matrices for 4 *div* and 12 *div*. *$p < 0.05$, **$p < 0.01$, ***$p < 0.001$. Comparisons were made using two-way ANOVA with Bonferroni's *post-hoc* test. Data represent mean ± SEM. For MTT, LDH and [^{3}H]-D-Asp uptake, n = 3 (4 *div*), n =

This article is protected by copyright. All rights reserved.

6 (12 *div*) from independent experiments. For total protein, n = 5 (4 *div*) and n = 9 (12 *div*) from independent experiments.

Figure 5 Effects of aligned and random PCL scaffolds on GFAP protein expression. (A) Western blot demonstrates a significant decrease in GFAP (51 kDa) protein expression after 12 *div* on both aligned and random PCL scaffolds. Samples from 3 independent experiments. β-actin (41 kDa) was used as loading control. Quantification was based on optical density, measured using ImageJ. Data represent mean ± SEM. **Significantly different from control, $p < 0.01$, one-way ANOVA with Dunnett's Multiple Comparison *post-hoc* test.

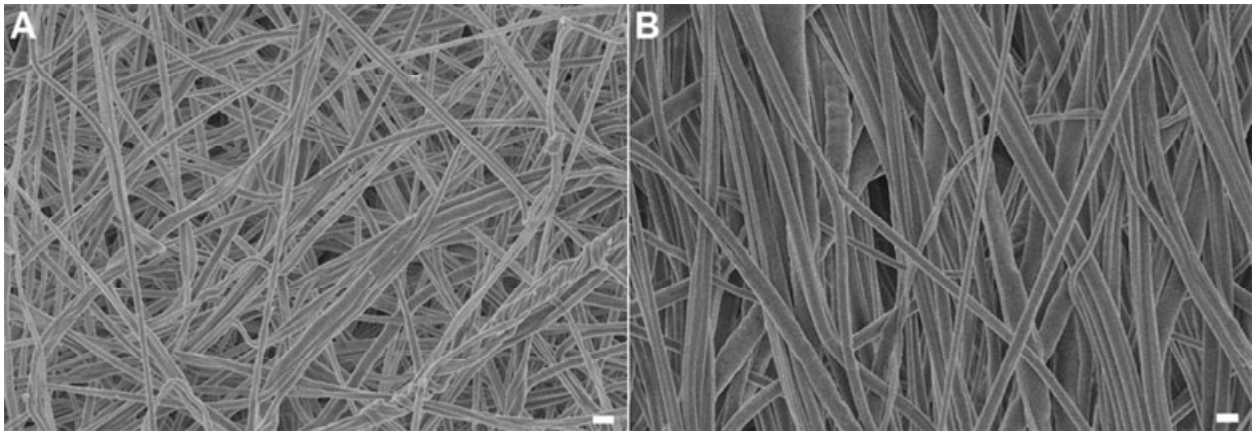
Figure 6 Three-Dimensional rendering of confocal images (Z-stacks). Astrocytes were grown for 12 *div* on (A) aligned PCL scaffold and (D) random PCL scaffold. (B), (C), (E) and (F) showed digital sectioning, revealing the cross section of the scaffold. Cells on the scaffold were labeled with GFAP (red) and Hoechst 33342 (blue). Divisions on x-/y-axes = 10 μm and on z-axis = 2 μm.

Figure 7 Expression profiles of selected genes when astrocytes were grown on different matrices for 12 *div* (C, control; P, 2D PCL; A, aligned scaffold; R, random scaffold). Data are presented as mean ± SEM from 4 independent experiments, and are expressed relative to the control. 95% confidence intervals were constructed for single-variate analysis where * indicates significant changes compared to control, $^{\#}$ indicates significant changes compared to 2D PCL.

This article is protected by copyright. All rights reserved.

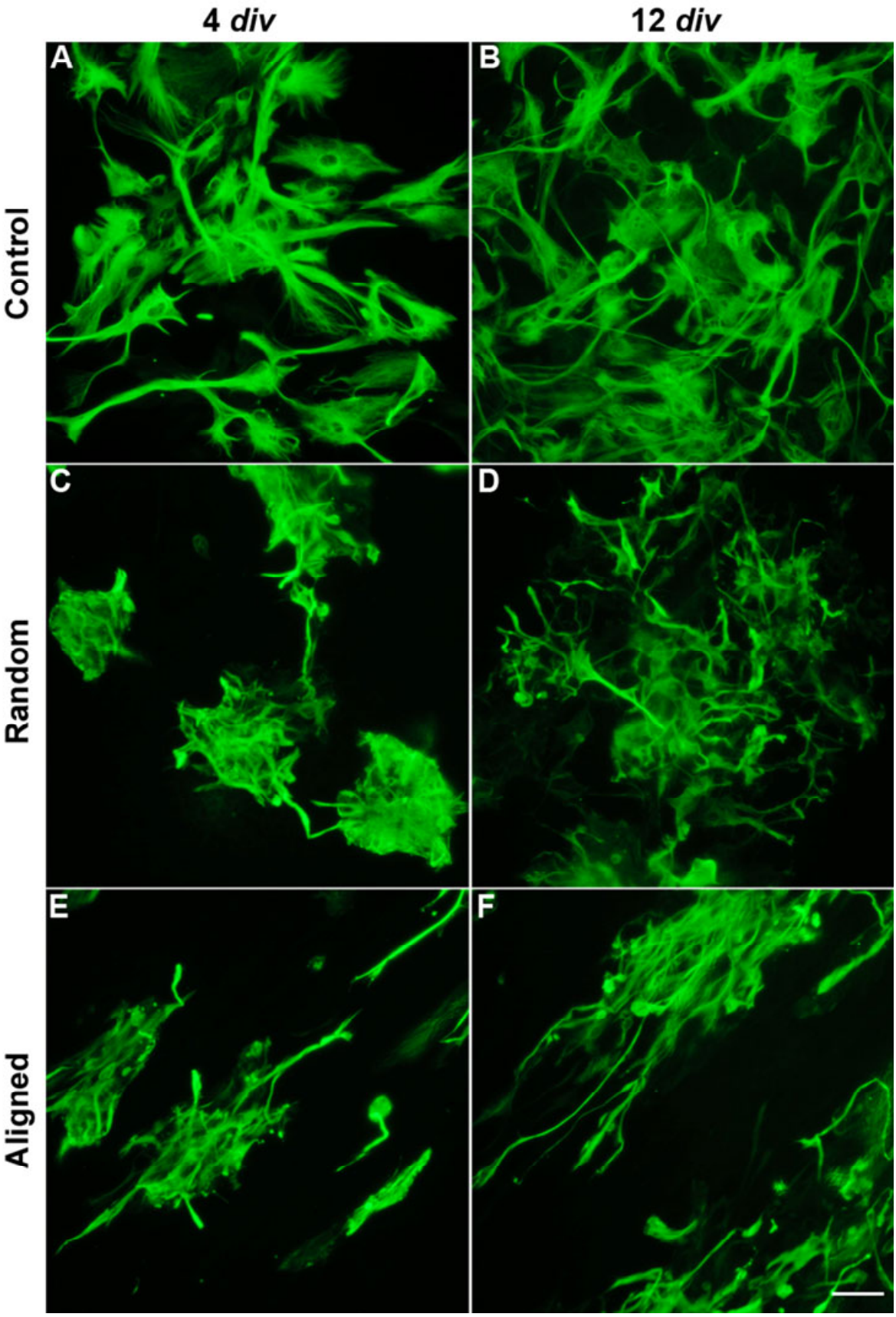
Accepted Article

Accepted Article



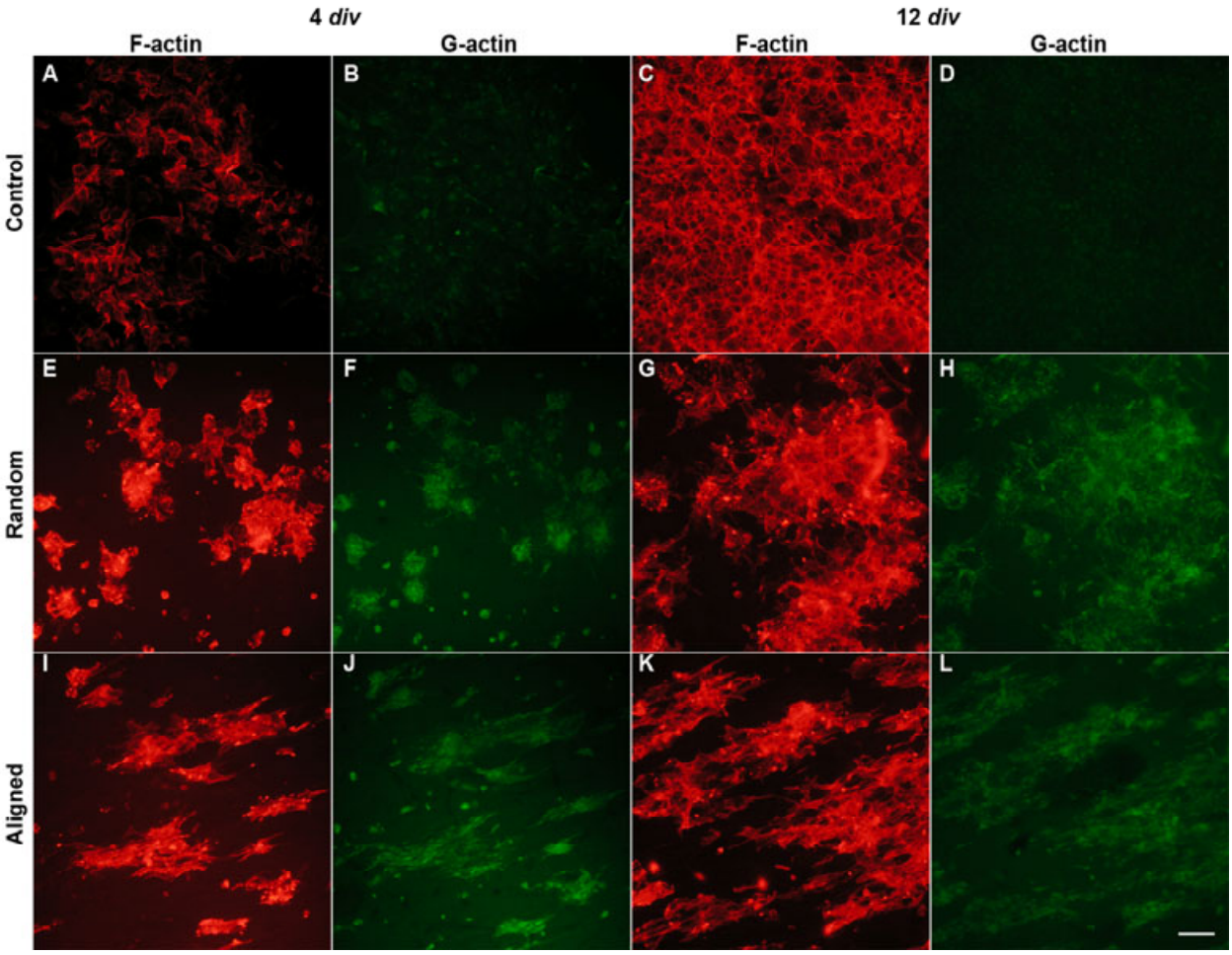
This article is protected by copyright. All rights reserved.

Accepted Article



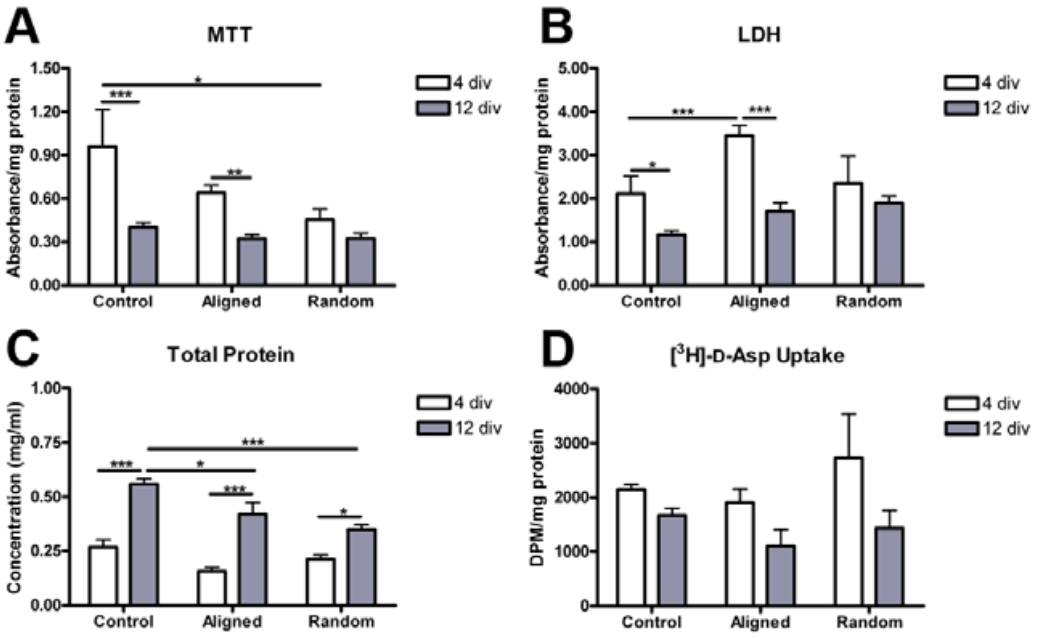
This article is protected by copyright. All rights reserved.

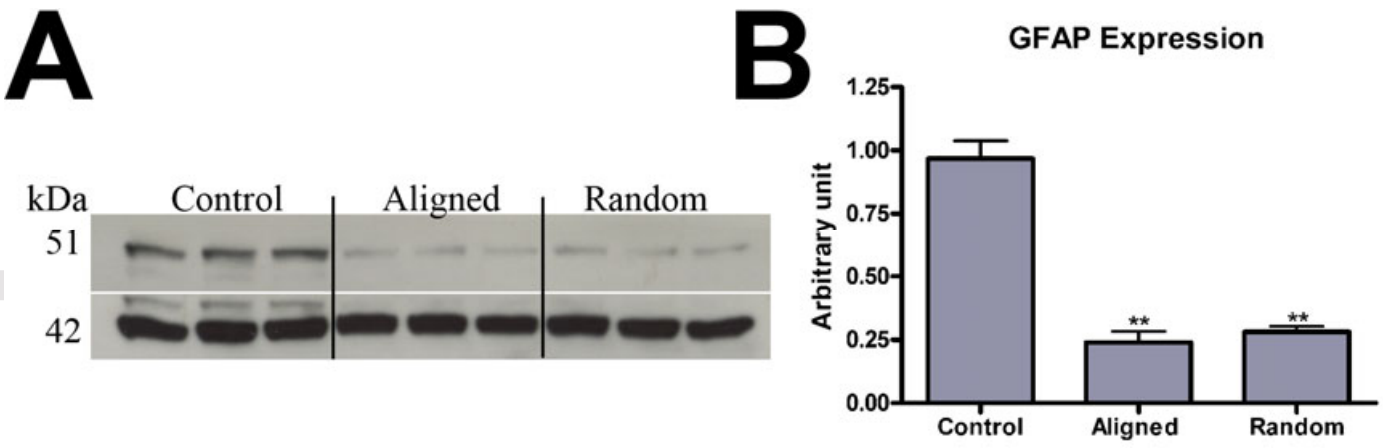
Accepted Article



This article is protected by copyright. All rights reserved.

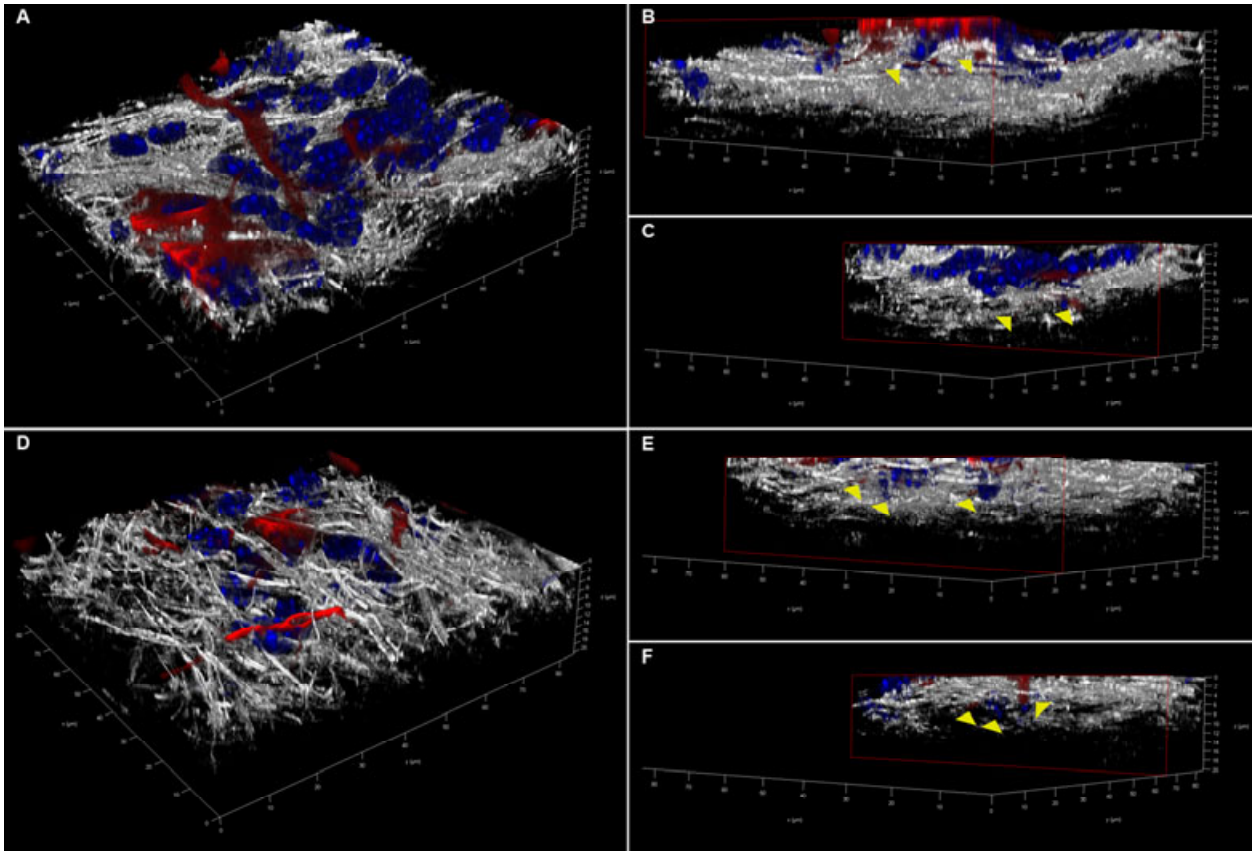
Accepted Article





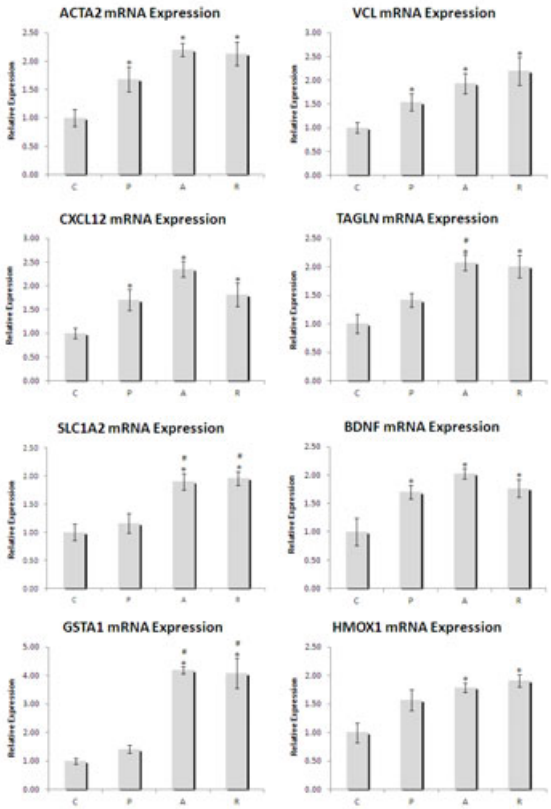
This article is protected by copyright. All rights reserved.

Accepted Article



This article is protected by copyright. All rights reserved.

Accepted Article



This article is protected by copyright. All rights reserved.